Critical x-ray scattering at the Peierls transition in the quasi-one-dimensional system $(TaSe_4)_2I$

Critical x-ray scattering at the Peierls transition in the quasi-one-dimensional system (TaSe$_4$)$_2$I

H Requardt†§, M Kalning†, B Burandt†, W Press† and R Currat‡

† Institut für Experimentalphysik, Universität Kiel, D-24098 Kiel, Germany
‡ Institut Laue–Langevin, 38042 Grenoble, France.

Abstract. By means of high-resolution x-ray scattering, we have studied the temperature dependence of the critical scattering associated with the Peierls transition in (TaSe$_4$)$_2$I. From a careful intensity and line shape analysis the critical exponents β, γ and ν were derived. β, γ and ν are the critical exponents of the temperature dependence of the order parameter, the susceptibility and the correlation length of the order parameter fluctuations, respectively. Though this incommensurate structural phase transition is reported to be continuous, an unusual exponent value is obtained: $\beta \approx 0.2$. The small value of β suggests a blurred first-order transition. We also report on the anisotropy of the correlation in the basal plane perpendicular to the (TaSe$_4$)$_\infty$-chain direction.

1. Introduction

One-dimensional metals undergo a phase transition, as predicted by Peierls [1], caused by an instability of the electron density. This instability generates a charge-density wave (CDW), which is accompanied by a modulation of the ionic positions in the lattice with wave vector $q = 2k_F$, where k_F is the Fermi wave number. This modulation is at the origin of the observed superstructure reflections. Up to now Peierls transitions have been found in a number of quasi-one-dimensional and quasi-two-dimensional systems. Such systems are often studied in connection with the highly anisotropic character of the electrical conductivity. Anisotropy ratios are typically of the order of 10^2–10^3 for conductivity values parallel and perpendicular to the chain direction.

The incommensurate distortion induced by the CDW leads to additional Bragg (satellite) reflections in the modulated (low-temperature) phase. The examination of the diffuse scattering above the phase transition temperature T_c offers the possibility of studying the criticality of the phase transition, as reflected by the temperature dependence of the intensity and correlation lengths both below and above T_c. For reviews on this subject see, e.g., [2, 3].

The compound under study here is (TaSe$_4$)$_2$I (space group $I422$), first investigated by Gressier *et al* [4]. It is composed of parallel chains (TaSe$_4$)$_\infty$ separated by strands of I atoms. It exhibits a Peierls transition at a temperature $T_c \approx 260$ K with an incommensurate modulation below the transition temperature. In this low-temperature phase the modulation leads to eight first-order satellite reflections in the vicinity of each main reflection, the positions of which are shown schematically in figure 1. The intensity distribution of the

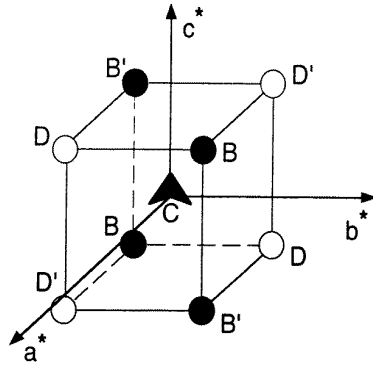§ Present address: Institut Laue–Langevin, 38042 Grenoble, France.

Figure 1. A sketch of the satellite positions in the vicinity of a main reflection. The triangle C represents the main reflection; the positions B and D indicate the eight first-order satellites (compare to [5]). The intensities of the satellites at B, B′ are higher than those at D, D′. Satellite B is stronger than satellite B′.

satellites is well described by the model of Lee *et al* [5]. In this model an acoustic-like harmonic CDW displacement $u(r)$ is assumed:

$$u(r) = \mu \sin(q \cdot r).$$

μ is the modulation amplitude vector, which is written as

$$\mu = \mu_\perp \left(\hat{a} - \frac{q_a}{q_b} \hat{b} \right) + \mu_\| \hat{c}$$

with $\mu_\perp = 0.087$ Å and $\mu_\| = 0.022$ Å at $T = 15$ K. $\hat{a}$, $\hat{b}$ and $\hat{c}$ are unit vectors along a, b and c. q_a, q_b are the components of the modulation wave vector q along the directions a and b, respectively. It is noticeable that Lee *et al* found the component $\mu_\|$ of the modulation amplitude along the chain direction to be smaller than the component $\mu_\perp$ perpendicular to the chains. With this modulation amplitude vector μ the intensity distribution $I(k)$ is calculated as

$$I(k) \propto [J_0(k \cdot \mu)]^2 \, \delta(k - G) + \sum_{n=1}^{\infty} [J_n(k \cdot \mu)]^2 \{\delta(k - G + nq) + \delta(k - G - nq)\}. \quad (1)$$

The intensity profiles and correlation lengths above the phase transition temperature were studied by Lorenzo and co-workers [6] by means of neutron diffraction. Since the Q-space resolution in neutron scattering experiments is rather limited, it was found desirable to perform high-resolution x-ray scattering experiments to obtain more detailed information close to the phase transition temperature.

   In this paper we present a high-resolution x-ray investigation of the critical scattering in the vicinity of the $(6\bar{2}0)$ main reflection. The measurements were carried out in a narrow temperature range extending both below and above T_c. The temperature dependences of the scattered intensities as well as of the correlation lengths were fitted to conventional power laws, in order to extract the critical exponents β, γ and ν. Similar work has been carried out on such other CDW compounds as blue bronze ($K_{0.3}MoO_3$) and NbSe₃ by Girault *et al* [7] and Moudden *et al* [8], respectively.

2. Experimental details

The $(6\bar{2}0)$ main reflection was chosen for this study since it provides a suitable intensity for the satellite reflections according to expression (1). The measurements were performed in Kiel on a three-crystal diffractometer [9] with a perfect Si(111) monochromator and analyser using Cu Kα_1 radiation from a 6.4 kW rotating anode RIGAKU RU200 (nominal power 12 kW). The instrument provides a resolution in the horizontal scattering plane of about $\Delta Q = 8 \times 10^{-4}$ Å^{-1} FWHM for scans along Q and about $\Delta Q' = 2 \times 10^{-4}$ Å^{-1} FWHM for the rocking direction. To match the line-shaped beam with the needle-shaped geometry of the sample ($0.8 \times 0.8 \times 5$ mm^3), with the long axis along the chain direction c^*, we chose the (a^*, b^*)-plane as the scattering plane. Because of the relaxed vertical resolution ($\Delta Q_Z = 5.7 \times 10^{-2}$ Å^{-1} FWHM) no attempt was made to extract profile widths along the c^*-axis.

A few scans were performed using a linear position-sensitive detector (PSD), mounted perpendicular to the scattering plane, instead of the NaI scintillation counter. The PSD makes use of the vertical resolution ΔQ_Z—sufficient to resolve the out-of-plane satellite pairs at $(6 \pm \Delta h, \bar{2} \pm \Delta k, \pm \Delta l)$. As shown below, however, the low count rate per channel of the PSD set-up precluded its use for the bulk of the present study.

For the sample under investigation, T_c was obtained from the power-law fits as 254.1 K (section 5) and measurements were performed between 248 K and 258 K. The temperature was scanned in steps of 0.5 K or 1 K using Peltier elements as cooling elements with a temperature accuracy of ± 0.1 K. The upper limit for the temperature range was found to be about 258 K, when the peak intensity of the diffuse scattering is reduced to only about twice the background level.

3. Measurements

The value of the modulation wave vector q_s was obtained from the positions of the satellite reflections as $q_s = (\pm \Delta h, \pm \Delta k, \pm \Delta l)$ with $\Delta h = \Delta k = 0.042\,56(8)$ and $\Delta l = 0.077(5)$ in reduced units, in close agreement with previous results [5, 10]. Here we investigated the critical scattering with $q_s = (-\Delta h, -\Delta k, \pm \Delta l)$ near the $(6\bar{2}0)$ main reflection. High-resolution scans were recorded in two directions in the basal (a^*, b^*)-plane: one along the direction $a^* + b^*$, which is parallel to the projection of q_s into the basal plane ($= q_s(a^*, b^*)$); the second, for technical reasons, not along the ideal direction perpendicular to $q_s(a^*, b^*)$, but along the vector Q, which gives an angle of about 60° between these scanning directions instead of 90°.

Figures 2(a) and 2(b) show the intensity profiles along the two scanning directions in the basal plane. At temperatures below T_c the profiles are slightly broader than the resolution function and their line shapes vary little with temperature. Above the phase transition temperature, in the critical fluctuation regime, the intensity profiles broaden rapidly and decrease in intensity with increasing temperature, until the diffuse intensity becomes hardly detectable. The line shapes of the critical scattering at $(-\Delta h, -\Delta k, -\Delta l)$ and $(-\Delta h, -\Delta k, +\Delta l)$, scanned with the PSD set-up along the chain direction c^* are shown in figure 3 for several temperatures above and below T_c. The intensity profiles exhibit two maxima centred at the two out-of-plane satellite positions. The vertical resolution is not sufficient for extraction of a c^* correlation length, as seen from the fact that the measured width of the peaks is independent of the temperature and identical to that of the $(6\bar{2}0)$ main reflection.
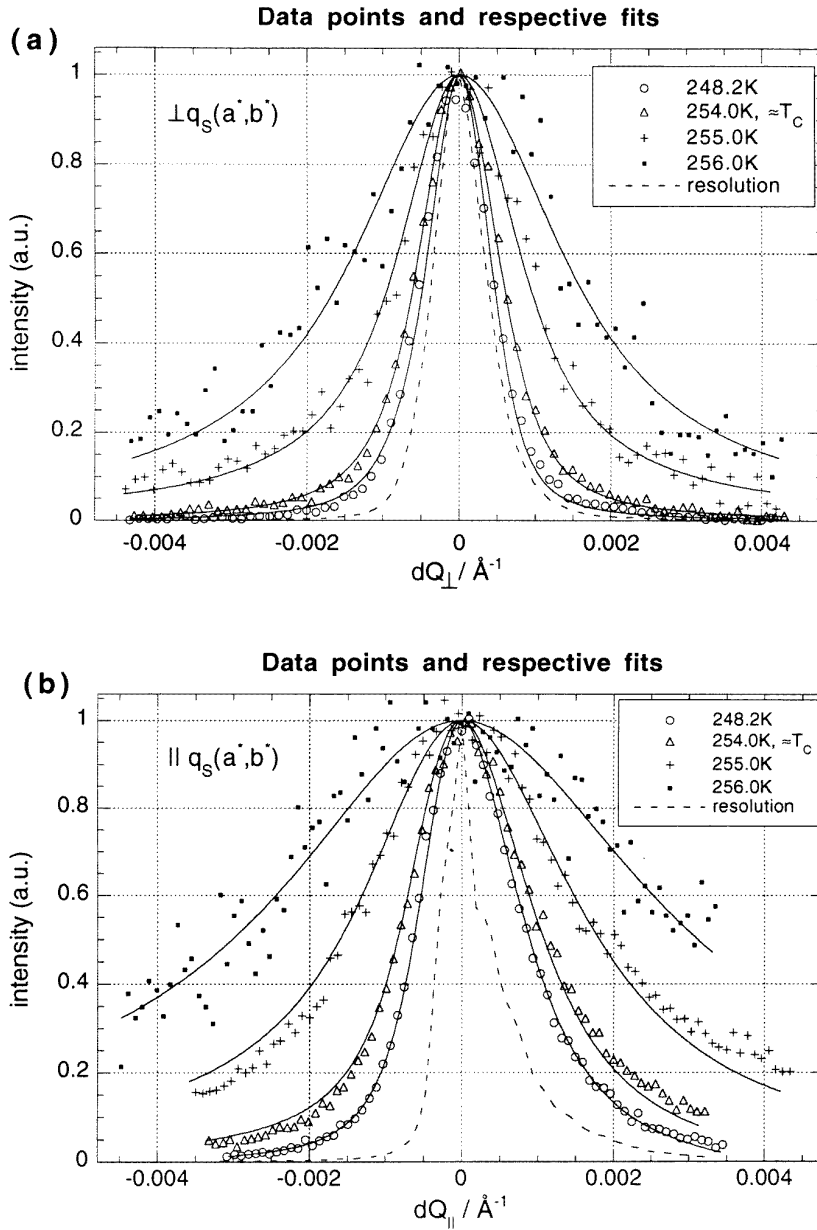
(a)

Data points and respective fits

(b)

Data points and respective fits

Figure 2. Critical scattering (symbols) and fits (full lines) for the scanning directions along Q (a) and parallel to $q_s(a^*, b^*)$ (b). The direction along Q is approximately perpendicular to $q_s(a^*, b^*)$; see the text, section 3. The broken lines in the figures refer to the intensity profiles of the main reflection taken as the instrumental resolution function.

4. Modelling the data

The intrinsic line shape of the diffuse scattering is described by the instantaneous correlation function
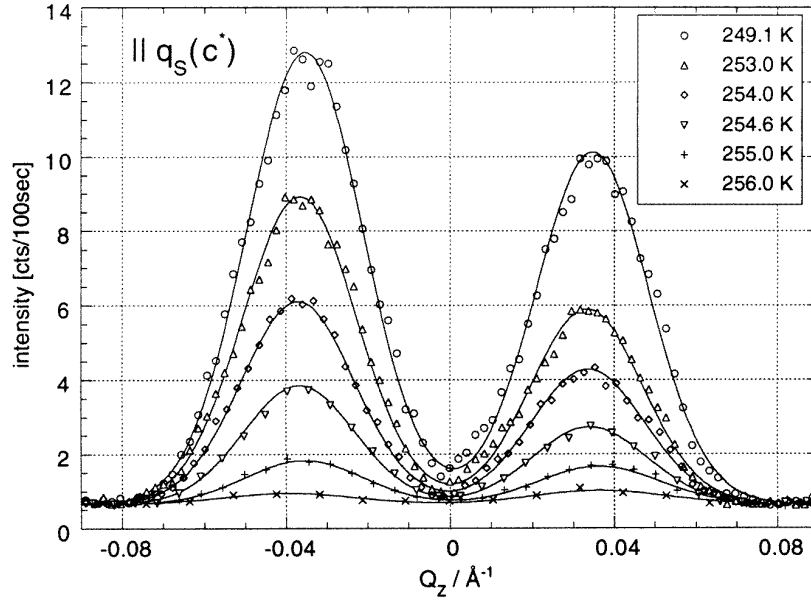
$$S(q) = k_B T \chi(q) \tag{2}$$

Figure 3. Critical scattering (symbols) and Gaussian fits (full lines) for the direction parallel to c^*, scanned with a position-sensitive detector (PSD) (see the text, section 3). Because of the low resolution these scans are not analysed with respect to correlation lengths.

where $\chi(q)$ is the susceptibility associated with the order parameter. In a simplified approach taking the scanning direction and the low-resolution direction into account, $\chi(q)$ is taken as a generalized Lorentzian profile with an exponent $1 < \Sigma < 2$ [11]:

$$\chi(q) \approx \chi(q_s) \left(\frac{1}{1 + \xi_1^2 \, \delta q_1^2 + \xi_2^2 \, \delta q_2^2} \right)^{\Sigma}. \tag{3}$$

The ξ_i are the correlation lengths of the fluctuations along these two directions. To model the measured intensity profiles, equation (2) with expression (3) is convoluted with the resolution function $R(q)$:

$$I(q) \propto \int S(q + \tau) R(\tau) \, \mathrm{d}\tau. \tag{4}$$

The resolution function $R(q)$ is approximated as

$$R(q) \approx R(q_1) \exp(-K^2 q_2^2).$$

Here direction 1 is taken to be the direction of the scan, the resolution profile of which is determined experimentally from the profile of the $(6\bar{2}0)$ main reflection. Direction 2 represents the low-resolution direction. From this convolution one gets for the intensity profile of the scanning direction

$$I(q_1) \approx I_0(q_s, T) \int R(\tau_1) \left(\frac{1}{1 + \xi_1^2 (q_1 + \tau_1)^2} \right)^{\Sigma - 1/2} \, \mathrm{d}\tau_1 \tag{5}$$

with $I_0(T)$ including all of the temperature dependence:

$$I_0(q_s, T) = \frac{I_0}{\xi_2(T)} k_B T \chi(q_s, T). \tag{6}$$

In figure 2 the fits of the intensity profiles with equations (5) and (6) are shown as full lines. The fits yield a value for the exponent $\left(\Sigma - \frac{1}{2}\right)$ in equation (5) of $\Sigma - \frac{1}{2} = 0.80 \pm 0.05$, i.e. a value of Σ well within the range of values given for equation (3).
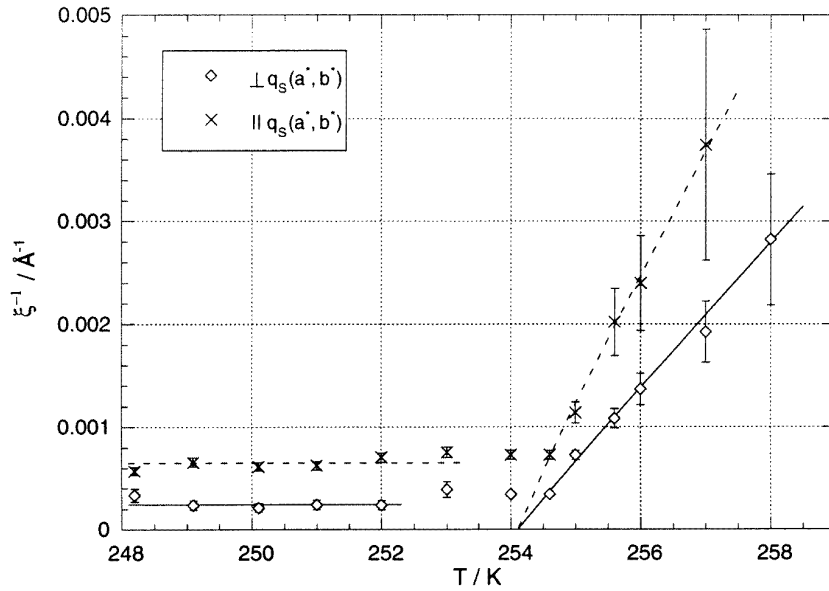

Figure 4. Reciprocal correlation lengths for the two scanning directions in the basal plane (a^*, b^*). The lines above T_c indicate the power-law fits. The lines below T_c represent mean values of the correlation lengths in the low-temperature phase.

5. Results

The temperature dependence of the correlation lengths and the intensities of the critical scattering below and above T_c were fitted with power laws:

$$\xi^{-1}(T) = \xi_0^{-1}\left(\frac{T - T_c}{T_c}\right)^{\nu} \tag{7}$$

$$\chi(q_s, T) = \chi_0(q_s)\left(\frac{T - T_c}{T_c}\right)^{-\gamma} \tag{8}$$

for $T > T_c$, giving with equations (6), (7) and (8) for the peak intensity above T_c:

$$\frac{I_0(q_s, T)}{T} \propto \left(\frac{T - T_c}{T_c}\right)^{-(\gamma - \nu_2)} \tag{9}$$

and for the integrated or peak intensity below T_c:

$$I_{int}(T) \propto \left(\frac{T_c - T}{T_c}\right)^{2\beta}. \tag{10}$$

From this we consistently obtained a value $T_c = 254.1 \pm 0.1$ K for the phase transition temperature. Note that expression (10) is valid only if the contribution from fluctuations below T_c can be neglected with respect to the satellite intensity. In that regime, we expect the

measured width of the intensity profiles to become temperature independent and resolution limited. However, we found that the measured profile widths saturate below $\approx(T_c - 1$ K) to a value which is slightly higher than the measured $(6\bar{2}0)$ width, taken as the effective instrumental width. This corresponds to finite values for the correlation lengths extracted from the measured intensity profiles, as shown in figure 4. This behaviour, which indicates a departure from true long-range order below T_c, is common to many incommensurate systems and arises from pinning of the modulation by defects as, e.g., reviewed in [2]. In practice, we have assumed that the effect of the dynamic fluctuations could be neglected below $T_c - 1$ K and restricted the power-law fit according to equation (10) to that temperature range.

The results from the fits for the temperature dependence of the correlation lengths are presented in figure 4. The present results complement the neutron data of Lorenzo and co-workers [6], from which a profile analysis close to T_c could not be extracted.

Table 1. Critical exponents of the temperature dependence of the correlation length (ν) and the integrated and peak intensity (exponents β and $\gamma - \nu_2$, respectively). (See equations (7)–(10) in the text.) ν_2 is the critical exponent assumed for the correlation length in the non-resolved c^*-direction.

Direction	Critical exponents			
	ν	β	$\gamma - \nu_2$	γ (with $\nu_2 = 1$)
$\parallel$ to $q_s(a^*, b^*)$ ($\parallel$ to $a^* + b^*$)	0.94 ± 0.10	0.22 ± 0.02	1.25 ± 0.13	2.25 ± 0.2
$\perp$ to $q_s(a^*, b^*)$ ($\parallel$ to Q)	0.98 ± 0.10	0.25 ± 0.02	1.49 ± 0.18	2.5 ± 0.3

Below T_c, we found mean values for the correlation lengths $\bar{d}$ in the modulated phase of $\bar{d}_\perp = 4100$ Å ± 400 Å for the direction along the scattering vector Q and $\bar{d}_\parallel = 1550$ Å ± 100 Å for the direction $a^* + b^*$—that is, parallel to $q_s(a^*, b^*)$. In figure 4 the full and broken line for $T < T_c$ indicate these mean values, respectively. These values lead to an anisotropy of $\bar{d}_\perp/\bar{d}_\parallel = 2.6 \pm 0.3$ for temperatures below T_c. Above T_c the reciprocal correlation lengths $\xi^{-1}(T)$ are fitted according to a power law. The results are indicated as lines in figure 4, and the values for the critical exponent ν are given in table 1. The values $\xi_{0,\perp} = 6.0$ Å ± 0.3 Å for the direction along Q and $\xi_{0,\parallel} = 4.1$ Å ± 1.7 Å for $a^* + b^*$, along $q_s(a^*, b^*)$, yield an anisotropy of $\xi_{0,\perp}/\xi_{0,\parallel} = 1.5 \pm 0.8$ in the basal plane, a small value, which is different from the anisotropy value found below T_c. However, such a small value is consistent with the results of Lorenzo and co-workers [6], who found no anisotropy in the basal plane. The discrepancy between the anisotropy values below and above T_c may be explained by the fact that the intensity profiles below T_c are at least partly controlled by the CDW domain sizes and texture.

The temperature dependence of the intensities is shown as a log–log plot in figures 5(a) and 5(b) for temperatures below and above T_c, respectively. For the critical exponent values β and γ, see table 1.

6. Discussion

The observed combination of critical exponents with a low β-value and a high γ-value (>2.3) is unusual and not predicted by a theoretical model for a continuous phase transition.
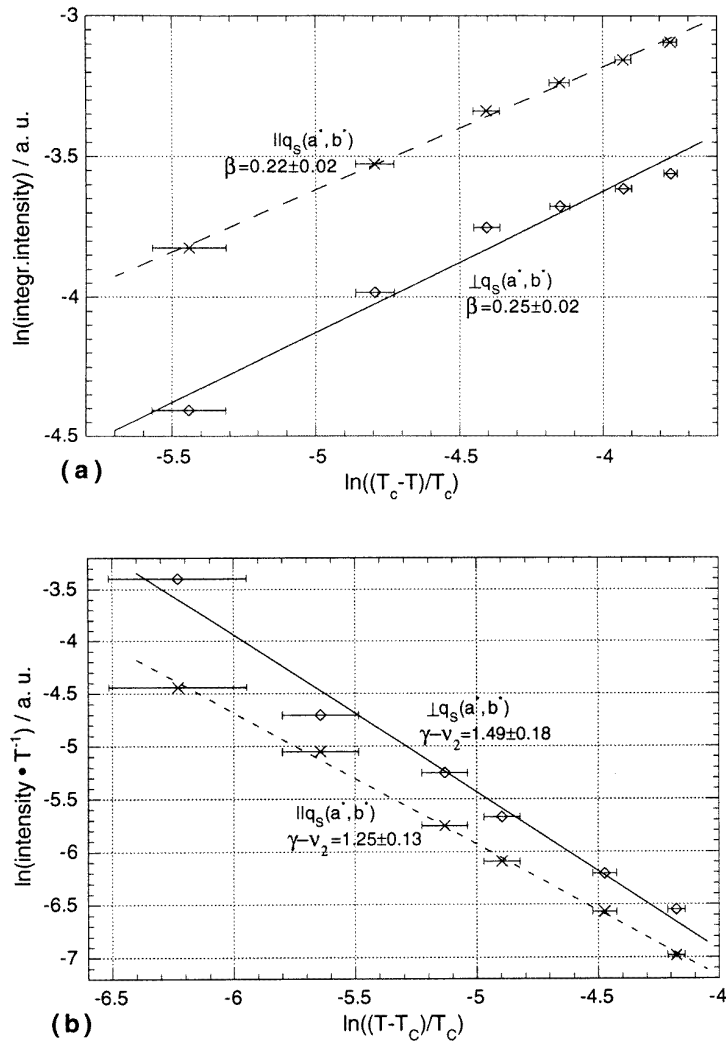
Figure 5. Log–log plots of the variation of the scattered intensity with reduced temperature. The temperature dependence of the integrated intensity $I_{int}(T)$ in the low-temperature phase is shown in (a). (b) displays the variation of the peak intensity $I_{peak}(T)/T$ in the regime of critical fluctuations. The lines indicate the power-law fits with the critical exponents β (a) and $\gamma - \nu_2$ (b) for the two scanning directions. For the latter see equation (9) in the text (section 5).

There are models giving high γ-values, like e.g. the spherical model ($\gamma = 2$) [12]. This model yields a value for ν ($\nu = 1$), also observed in our experiment, but predicts a much higher value for β: $\beta = \frac{1}{2}$.

Most remarkable yet is the value of $\beta \approx 0.2$. This rather low value is in agreement with the results of Lorenzo and co-workers [6], who found $2\beta = 0.37 \pm 0.01$ from neutron scattering. Models for continuous phase transitions predicting such low values for β do exist: e.g., transitions close to a Lifshitz point or a tricritical point, where the crossover due to the vicinity of such points leads to effective β-values of about 0.18 [13]. Another model predicting low β-values is, e.g., the two-dimensional Ising model with a β of $\frac{1}{8}$, even

lower than that observed in our experiment. Nevertheless, these models seem unlikely to be applicable to $(TaSe_4)_2I$, since on the one hand the existence of a Lifshitz point or a tricritical point is not known for this compound, and on the other hand the observed anisotropy of the correlation lengths of the fluctuations do not hint at a two dimensionality of the system.

A possible interpretation of the low β-value could be that the phase transition is not continuous but is in fact a blurred discontinuous transition, although there is as yet no other evidence for a first-order character of the phase transition in $(TaSe_4)_2I$. Commensurability with the parent lattice, which may lead to a discontinuous transition, has not been observed in $(TaSe_4)_2I$ so far.

As, e.g., Hüller and Press [14] and Dorner and Comès [15] have shown, treating a phase transition, which is of first order within mean-field (MF) theory, with conventional power laws as for a continuous one, may lead to apparent values for β between $\frac{1}{6}$ and $\frac{1}{4}$. In the framework of this approach, with the mean-field transition temperature T_{MF} lower than the actual phase transition temperature T_c, one should expect an apparent value for γ lower than 1, although this has not been calculated. This estimated γ-value does not correspond to our results with a value for γ higher than 2, which hints at the importance of fluctuations in $(TaSe_4)_2I$.

Aharony and Blankschtein [16] have given another approach: a phase transition, continuous within MF theory, as normally expected for transitions to an incommensurate state, can be driven to be discontinuous by fluctuations if the order parameter has more than four components. In this case, T_{MF} is assumed to be higher than T_c, so one can expect an apparent γ-value higher than 1 in the case of a blurred first-order transition. For the exponent β one can expect a value similar to that given by [14, 15]. Since the order parameter of $(TaSe_4)_2I$ has eight components, this could be the explanation for the discontinuous nature of the transition.

Another hint strengthening our interpretation of the phase transition can be seen in figure 4. For a continuous transition and weak pinning at low temperatures one could expect an increase in $\xi^{-1}(T)$ when approaching T_c from below, due to a change of the pinning from weak to strong. The fact that within the limits of the observed data points no such increase in $\xi^{-1}(T)$ is evident can be seen as supporting the interpretation as a blurred discontinuous phase transition.

7. Conclusion

We have been able to follow the temperature dependence of the intensity profiles of the critical scattering in the low-temperature phase ($T < T_c$) and in the regime of fluctuations ($T > T_c$) in a narrow temperature range close to the phase transition temperature T_c. Measurements with high Q-resolution in the basal plane (a^*, b^*) perpendicular to the chain direction were performed, allowing us to obtain from the intensity profiles the correlation length of the fluctuations above T_c and finite correlation lengths below the phase transition temperature. The anisotropy of the fluctuations ($T > T_c$) is consistent with previous neutron scattering measurements. Below T_c, we found an asymmetry for the two scanning directions, which was ascribed to the influence of CDW domain size and texture. We also derived critical exponents β and γ from the temperature variations of the integrated and peak intensity of the critical scattering, respectively, and ν from the correlation lengths of the fluctuations. These quantitative observations suggest a blurred discontinuous phase transition of the compound $(TaSe_4)_2I$ at T_c in contrast to the usually continuous incommensurate phase transitions.

In the present study we could not explore the direction c^* along the chains, due to

the limited instrumental resolution along this scanning direction. Since the direction c^* is the quasi-one-dimensional direction, it should exhibit the strongest correlation of the modulation. It is planned to investigate the direction along the chains at a synchrotron source in order to complete this study.

Acknowledgments

References

[1] Peierls R E 1955 *Quantum Theory of Solids* (Oxford: Clarendon) p 108
[2] Grüner G 1988 The dynamics of charge density waves *Rev. Mod. Phys.* **60** 1129; 1994 Density waves in solids *Frontiers in Physics* vol 89 (New York: Addison-Wesley)
[3] Monceau P (ed) 1985 *Electronic Properties of Inorganic Quasi-One-Dimensional Compounds* (Dordrecht: Reidel)
[4] Gressier P, Guemas L and Meerschaut A 1982 Preparation and structure of ditantalum iodine octaselenide, Ta_2ISe_8 *Acta Crystallogr.* B **38** 2877
[5] Lee K-B, Davidov D and Heeger A J 1985 X-ray diffraction study of the CDW phase in $(TaSe_4)_2I$: determination of the CDW modulation amplitude *Solid State Commun.* **54** 673
[6] Lorenzo J E 1992 *PhD Thesis* ILL, Grenoble
    Lorenzo J E, Currat R, Monceau P, Hennion B and Levy F 1993 Neutron study of the Peierls transition and the low frequency excitations in $(TaSe_4)_2I$ *J. Physique Coll.* IV **3** C2 209
    Lorenzo also investigated the plane $(c^*, a^* + b^*)$, for which he found a value of the anisotropy of the correlation lengths of 1.8, consistent with former results of Fujishita *et al* [10] for the isomorphous compound $(NbSe_4)_2I$.
[7] Girault S, Moudden A H and Pouget J P 1989 Critical x-ray scattering at the Peierls transition of the blue bronze *Phys. Rev.* B **39** 4430
[8] Moudden A H, Axe J D, Monceau P and Levy F 1990 q_1 charge density wave in $NbSe_3$ *Phys. Rev. Lett.* **65** 223
[9] Brügemann L 1989 *PhD Thesis* Christian Albrechts University, Kiel
[10] Fujishita H, Sato M, Sato S and Hoshino S 1985 X-ray diffraction study of the quasi-one-dimensional conductors $(MSe_4)_2I$ (M = Ta and Nb) *J. Phys. C: Solid State Phys.* **18** 1105
[11] Lorenzo J E, The problem of the convolution of the Lorentzian and the Lorentzian squared cross section with the resolution, unpublished
[12] Stanley H E 1971 *Introduction to Phase Transitions and Critical Phenomena*. (Oxford: Clarendon)
[13] Folk R and Moser G 1993 Lifshitz points in uniaxial ferroelectrics *Phys. Rev.* B **47** 13 992
[14] Hüller A and Press W 1979 Theoretical aspects of solid rotator phases *The Plastically Crystalline State* ed J N Sherwood (New York: Wiley)
[15] Dorner B and Comès R 1977 Phonons and structural phase transformations *Springer Topics in Current Physics* vol 3 (Berlin: Springer) and references therein
[16] Aharony A and Blankschtein D 1982 Multicritical phenomena in structural phase transitions *Phys. Scr.* T **1** 53